Chapter 2

Magnetic Properties

In the preceding introductory chapter we focused more on the electrical property of a superconductor that its electrical resistance ρ vanishes below a critical temperature T_c. In the following we discuss that a superconductor differs from an ideal conductor as its magnetic properties are additionally decisive. Namely, it turns out that a superconductor also represents an ideal diamagnet as it expels magnetic flux lines.

2.1 Meissner Ochsenfeld Effect

An ideal conductor is described by the Maxwell equations in matter with a vanishing electrical resistance ρ. From this we can draw the following two conclusions:

- According to the Ohm law, which is a matter equation, the current density $\mathbf{j}$ is proportional to the electric field $\mathbf{E}$

$$\mathbf{j} = \sigma\, \mathbf{E} \tag{2.1}$$

  with the conductivity $\sigma = 1/\rho$ being the proportionality constant. Thus, in the limit of a vanishing resistance ρ we obtain

$$\lim_{\rho \to 0} \mathbf{E} = \lim_{\rho \to 0} \rho\, \mathbf{j} = \mathbf{0}\,. \tag{2.2}$$

- The inductivity law, which is a consequence of the Maxwell equations, the vortex density of the electric field $\mathbf{E}$, i.e. $\operatorname{rot} \mathbf{E}$, is determined by the time derivative of the magnetic induction $\mathbf{B}$

$$\operatorname{rot} \mathbf{E} = -\frac{\partial \mathbf{B}}{\partial t}\,, \tag{2.3}$$

  where the additional minus sign represents the Lenz law. Inserting (2.2) into (2.3) yields

$$\lim_{\rho \to 0} \frac{\partial \mathbf{B}}{\partial t} = \mathbf{0}\,, \tag{2.4}$$

i.e. the magnetic induction does not change temporally:

$$\mathbf{B}(t) = \text{ const.}\,. \tag{2.5}$$

Physically this means that in the loop of an ideal conductor with fixed area we do not have any induction voltage as the magnetic flux through it does not change.

But in contrast to (2.4) Meissner and Ochsenfeld discovered experimentally in 1933 that the magnetic induction $\mathbf{B}$ vanishes inside a superconductor:

$$\mathbf{B} = \mathbf{0}\,. \tag{2.6}$$

This finding differs from (2.5) and can not be explained within the realm of classical physics. In order to understand this better, we compare now the behavior of an ideal conductor with the one of a superconductor within a gedanken experiment. To this end we consider a cycle process within the B-T phase diagram as shown in Fig. 2.1a). For simplicity we restrict ourselves to a spherical body as it can be shown that the magnetic field inside is homogeneous, see Sec. 2.4 below. According to the very left of Fig. 2.1b) we compare the two different cases that the cycle process of Fig. 2.1a) occurs clockwise (upper row) or counterclockwise (lower row), respectively. For the clockwise cycle process we observe that the field lines of the magnetic induction turn out to coincide for both ideal conductor and superconductor despite the different underlying laws (2.5) and (2.6). But for the counterclockwise cycle process we conclude from (2.5) and (2.6) that the field lines of the magnetic induction differ for the ideal conductor and the superconductor at point c and b. With this we can draw the following far-reaching conclusions:

- The Meissner-Ochsenfeld effect guarantees that a state in a superconductor is path independent. Therefore, it is possible to describe superconductivity within the phenomenological approach of thermodynamics as is discussed in Chap. 3.

- As the behavior of a superconductor differs from an ideal conductor, the superconducting state cannot only be described by the Maxwell equations alone. They must be generalized by the London equations as is worked out in Chap. 4.

Let us briefly mention the physical origin of the Meissner-Ochsenfeld effect. It stems from the fact that within a skin of about 100 Å at the surface of a superconductor currents of Cooper pairs persist. Due to the mobility of the Cooper pairs their currents adjust themselves such that the magnetic field vanishes inside the superconductor. In that sense one can call a superconductor an ideal diamagnet.

2.2 Type I Superconductor

A superconductor of type I has two phases according to Fig. 2.2, see also Fig. 1.7. The superconducting phase ① shows in the volume the Meissner-Ochsenfeld effect, whereas the other one

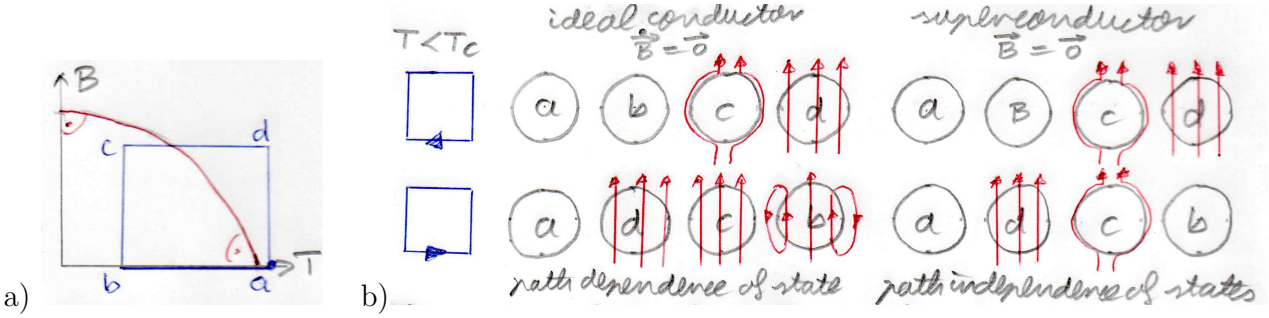

Figure 2.1: Gedanken experiment: a) Cycle process within the B-T phase diagram. b) Comparing magnetic properties of an ideal conductor in (2.4) with a superconductor in (2.6).

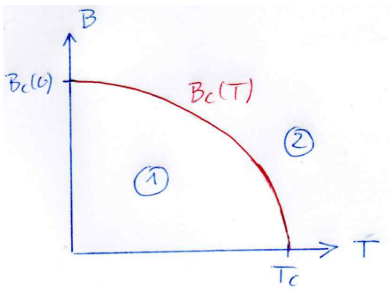

Figure 2.2: Phase diagram of type I superconductor.

② represents the normal conducting phase. Note that the transition line between both phases is described in good approximation by the formula of Kok (1.3). Furthermore, we remark that we neglect in the following discussion the shape of the body, which usually leads to an additional stray field. As we will see below in Sec. 2.4, this corresponds approximately to the situation of an infinitely long cylinder. In matter the magnetic induction $\mathbf{B}$ consists of two contributions:

$$\mathbf{B} = \mathbf{B}_{\text{ext}} + \mathbf{B}_{\text{int}} \,. \tag{2.7}$$

The first one comes from the magnetic field $\mathbf{H}$ imposed from outside

$$\mathbf{B}_{\text{ext}} = \mu_0 \, \mathbf{H} \,, \tag{2.8}$$

where μ_0 denotes the vacuum permeability. The second one describes the impact of matter in terms of the magnetization $\mathbf{M}$, which stems from the alignment of the elementary magnets in the volume. In case that we have an infinitely large volume we have

$$\mathbf{B}_{\text{int}} = \mu_0 \, \mathbf{M} \,. \tag{2.9}$$

The Lorentz force of a magnetic field upon a moving electrical charge depends on the magnetic induction $\mathbf{B}$. Thus, the Lorentz force does not discriminate whether the physical origin of the magnetic field stems externally from $\mathbf{H}$ or internally from $\mathbf{M}$.

In matter the magnetization $\mathbf{M}$ is proportional to the external magnetic field $\mathbf{H}$, which defines the magnetic susceptibility χ_{m}:

$$\mathbf{M} = \chi_{\text{m}} \, \mathbf{H} \,. \tag{2.10}$$

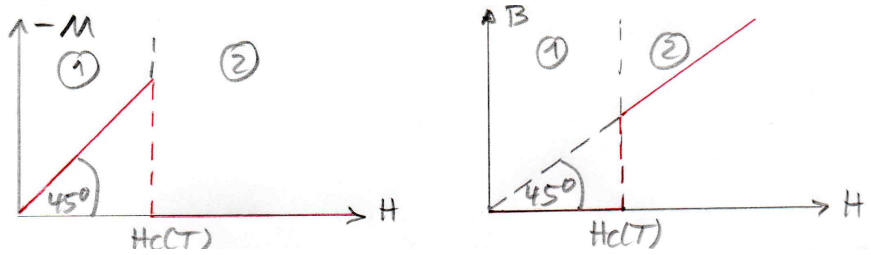

Figure 2.3: Negative magnetization and magnetic induction as function of magnetic field for type I superconductor.

element	abbreviation	atomic number	$B_c(0) = \mu_0 H_c(0)$ in T
lead	Pb	82	0.0803
tantalium	Ta	73	0.0830
aluminium	Al	13	0.0990
vanadium	V	23	0.131

Table 2.1: Critical magnetic fields of selected type I superconductors.

Thus from (2.7)–(2.10) we conclude

$$\mathbf{B} = \mu_0(1 + \chi_\mathrm{m})\,\mathbf{H}\,. \tag{2.11}$$

The Meissner-Ochsenfeld effect (2.6) has then the consequence that the magnetic susceptibility of a superconductor is fixed by

$$\chi_\mathrm{m} = -1\,. \tag{2.12}$$

This is the defining property of an ideal diamagnet.

In contrast to that the magnetic susceptibility in the normal conducting state stems from paramagnetism. Typically this leads to a value of about $\chi_\mathrm{m} \approx 10^{-5}$, which is negligibly small in comparison to (2.12). Thus, we have approximately in the normal conducting state

$$\chi_\mathrm{m} \approx 0\,. \tag{2.13}$$

The results (2.12) and (2.13) can now be summarized by corresponding magnetization curves. Here two representations are possible, either one plots the negative magnetization or the magnetic induction as a function of the magnetic field as is shown in Fig. 2.3. For the sake of concreteness we present in Tab. 2.1 some examples of type I superconductors together with their respective critical magnetic fields at zero temperature. From this table we conclude that the critical magnetic fields of type I superconductors are generically small.

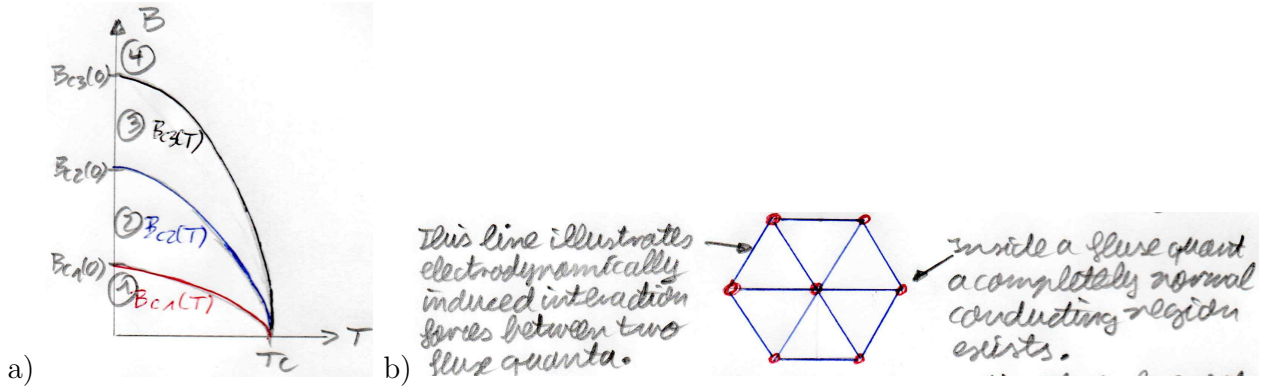

Figure 2.4: Type II superconductor: a) Phase diagram. b) Hexagonal lattice of flux lines in Shubnikov phase ②.

2.3 Type II Superconductor

A superconductor of type II has in total four phases in the B-T plane of control parameters, see Fig. 2.4a). The Meissner phase ① shows in the volume the Meissner-Ochsenfeld effect. There the magnetic flux is completely expelled from the superconductor. The Shubnikov phase ② represents a mixed state, where a hexagonal lattice of flux lines exists, see Fig. 2.4b). In the surface phase ③ superconductivity only exists at the surface. And ④ represents the normal conducting phase.

Note that the four phases are separated by three transition lines. Here $B_{c1}(T)$, $B_{c2}(T)$, $B_{c3}(T)$ are called lower and upper critical magnetic field as well as critical magnetic field of surface superconductivity, respectively. All three of them follow the Kok approximation (1.3) with the same critical temperature T_c:

$$\frac{B_i(T)}{B_{ci}(0)} = 1 - \left(\frac{T}{T_c}\right)^2 ; \quad i = 1, 2, 3\,. \tag{2.14}$$

Let us now describe in more detail the respective magnetic properties of all four phases:

① Meissner phase at $0 \leq B \leq B_{c1}(T)$:
Here we have weak diamagnetism, which is characterized by (2.12).

② Shubnikov phase at $B_{c1}(T) \leq B \leq B_{c2}(T)$:
With increasing the external magnetic field strength the number of flux lines also increases. As the inner region of each flux line is normal conducting, i.e. we have there $\chi_m = 0$, the total normal region increases. This has the consequence that the magnetization M decreases with increasing the external magnetic field.

③ Surface phase at $B_{c2}(T) \leq B \leq B_{c3}(T)$:
As the whole volume is already superconducting, the magnetization is already zero, i.e. we have $M = 0$.

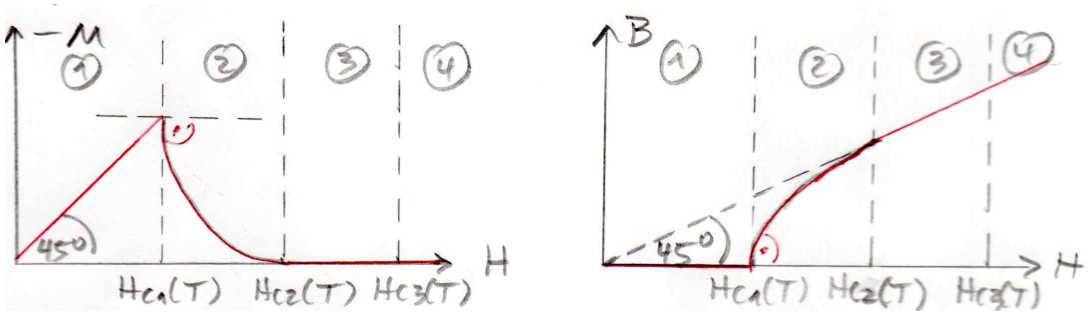

Figure 2.5: Negative magnetization and magnetic induction as function of magnetic field for type II superconductor.

material	Nb	NbTi	Nb_3Sn	$YBa_2Cu_3O_7$
$B_{c_2}(0) = \mu_0 H_{c_2}(0)$ in T	0.1944	14	25	$\sim 10^2$

Table 2.2: Critical magnetic fields of selected type II superconductors.

④ Normal conducting phase at $B_{c3}(T) \leq B$:
Here we have paramagnetism, which yields for all practical purposes $\chi_m = 0$.

Also for type II superconductors there are two possible representations for magnetization curves as is illustrated in Fig. 2.5. Some examples of type II superconductors together with their upper critical magnetic fields at zero temperature are listed in Tab. 2.2. Thus, we conclude that the critical magnetic fields of type II superconductors are larger than the critical magnetic fields of type I superconductors from Tab. 2.1. Therefore, type I (II) superconductors are called soft (hard) superconductors.

2.4 Description of Complete Diamagnetism

Here we investigate how the shape of the probe affects the magnetization curves of type I superconductors.

2.4.1 Physical Picture

To this end we start with describing the underlying physical picture by the example of a homogeneous sphere of a superconducting material:

1. In Fig. 2.6a) the sphere is put into an external magnetic field $\mathbf{B}_{ext} = \mu_0 \mathbf{H}$.

2. At the surface of the sphere surface currents of superconducting Cooper pairs emerge, see Fig. 2.6b). This leads to a magnetization $\mathbf{M}$, which is pointing opposite to the external magnetic field $\mathbf{H}$ due to the diamagnetic property of the superconductor.

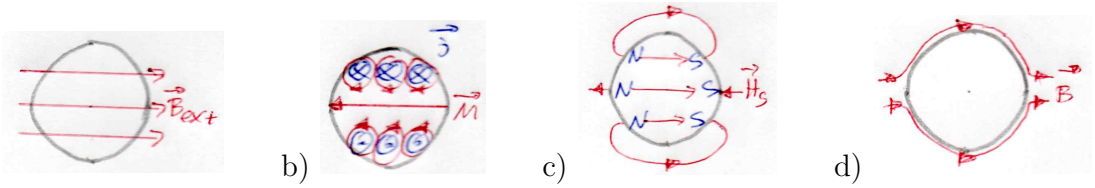

Figure 2.6: Homogeneous sphere of a superconducting material in an external magnetic field.

3. Due to the magnetization $\mathbf{M}$ effective magnetic charges emerge at the surface of the sphere. As the magnetization $\mathbf{M}$ is pointing from the south pole to the north pole, a stray field $\mathrm{H_s}$ emerges as indicated in Fig. 2.6c) which points inside the sphere parallel to the external magnetic field.

4. Superimposing all three field contributions yields a magnetic induction $\mathbf{B}$ in agreement with the Meissner-Ochselfeld effect as shown in Fig. 2.6d).

2.4.2 Stray Field

Now we describe this situation quantitatively. Again the magnetic induction $\mathbf{B}$ decomposes according to (2.7) with the external magnetic field (2.8). But now we have to generalize (2.9), which is only valid for an infinitely large volume, to a finite probe:

$$\mathbf{B}_{\mathrm{int}} = \mu_0 \left(\mathbf{M} + \mathbf{H}_{\mathrm{s}} \right) . \tag{2.15}$$

Here the stray field $\mathbf{H}_{\mathrm{s}}$, which is also called demagnetization field, is discussed in more detail, for instance, in Refs. [1, 2]. For a homogeneous magnetization $\mathbf{M}$ inside the probe the resulting stray field $\mathbf{H}_{\mathrm{s}}$ is given by

$$\mathbf{H}_{\mathrm{s}} = -N\,\mathbf{M} . \tag{2.16}$$

Thus, the minus sign guarantees that $\mathbf{H}_{\mathrm{s}}$, which originates from a surface effect, points opposite to the magnetization $\mathbf{M}$, which stems from a volume effect. Furthermore, N denotes the demagnetization tensor, whose components are given by

$$N_{ij} = \frac{-1}{4\pi} \int_{\partial V} dF'_j \, \frac{\partial}{\partial x'_i} \, \frac{1}{|\mathbf{r} - \mathbf{r}'|} \tag{2.17}$$

with the integral encompassing the whole surface ∂V of the volume V of the probe. For a homogeneous stray field the integral (2.17) yields a demagnetization tensor which does not depend on the position $\mathbf{r}$. Note the useful property that the trace over the demagnetization tensor is always unity:

$$\begin{aligned} \mathrm{Tr}\, N &= N_{ii} = \frac{-1}{4\pi} \int_{\partial V} dF'_i \, \frac{\partial}{\partial x'_i} \frac{1}{|\mathbf{r} - \mathbf{r}'|} = \frac{-1}{4\pi} \int_{\partial V} d\mathbf{F}' \, \boldsymbol{\nabla}' \frac{1}{|\mathbf{r} - \mathbf{r}'|} \\ &= \frac{-1}{4\pi} \int_V dV' \, \Delta' \frac{1}{|\mathbf{r} - \mathbf{r}'|} = \int_V dV' \, \delta(\mathbf{r} - \mathbf{r}') = 1 . \end{aligned} \tag{2.18}$$

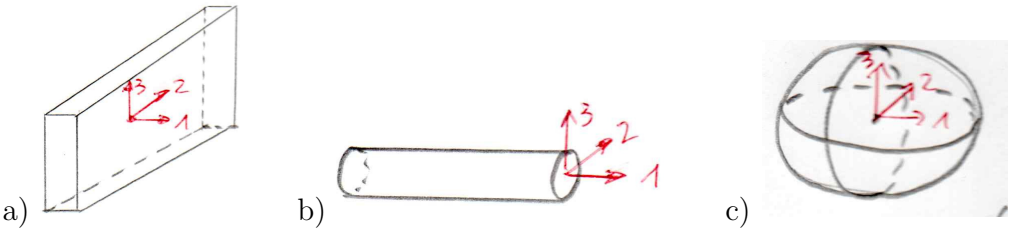

Figure 2.7: Different probe shapes with symmetries, for which the demagnetization tensor can be directly read off due to the trace property (2.18).

Here we have used the Gauß law and the fact that the Coulomb potential is the Green function of the Poisson equation of electrostatics. And, finally, we took into account that the coordinate $\mathbf{r}$ is inside the volume V.

In principle, the matrix elements of the demagnetization tensor N_{ij} can be directly calculated for each probe by evaluating the integral (2.17). However, the trace property (2.18) together with symmetry arguments can be used to determine straight-forwardly the demagnetization tensor. Let us illustrate this procedure by the following probe shapes:

1. Infinitely thin layer, see Fig. 2.7a):
   Here we have $N_2 = N_3 = 0$, as the magnetic surface charges vanish at infinity, which yields together with the trace property $N_1 + N_2 + N_3 = 1$ the result $N_1 = 1$. Thus, the demagnetization tensor reads

$$N = \begin{pmatrix} 1 & 0 & 0 \\ 0 & 0 & 0 \\ 0 & 0 & 0 \end{pmatrix} . \tag{2.19}$$

2. Infinitely long cylinder, see Fig. 2.7b):
   On the one hand we have $N_1 = 0$ analogous to the infinitely thin layer case, on the other hand the symmetry demands $N_1 = N_3$. From the trace property $N_1 + N_2 + N_3 = 1$ we then conclude $N_1 = N_2 = 1/2$, which leads to the demagnetization tensor

$$N = \begin{pmatrix} 0 & 0 & 0 \\ 0 & 1/2 & 0 \\ 0 & 0 & 1/2 \end{pmatrix} . \tag{2.20}$$

3. Sphere, see Fig. 2.7c):
   Due to symmetry all diagonal elements of the demagnetization tensor coincide, i.e. $N_1 = N_2 = N_3$. From the trace property $N_1 + N_2 + N_3 = 1$ we deduce consequently $N_1 = N_2 = N_3 = 1/3$ with the demagnetization tensor

$$N = \begin{pmatrix} 1/3 & 0 & 0 \\ 0 & 1/3 & 0 \\ 0 & 0 & 1/3 \end{pmatrix} . \tag{2.21}$$

With this we are equipped to study how the probe shape affects the Meissner-Ochsenfeld effect. To this end we insert (2.8), (2.15), and (2.16) into (2.7) for a particular direction of the external magnetic field

$$B = \mu_0 \, (H + M - NM) \, . \tag{2.22}$$

As the magnetic induction has to vanish inside the probe due to the Meissner-Ochsenfeld effect (2.6), we conclude:

$$M(H) = -\frac{1}{1-N} \, H \, . \tag{2.23}$$

Due to (2.10) the slope of the magnetization M with respect to the magnetic field H defines the magnetic susceptibility, so we deduce from (2.23)

$$\chi_{\mathrm{m}} = \frac{\partial M(H)}{\partial H} = -\frac{1}{1-N} \, . \tag{2.24}$$

Thus, we read off from (2.24) that the probe shape and, therefore, the demagnetization N leads to an increase of the absolute value of the magnetic susceptibility. As the demagnetization N is limited due to the trace property (2.18) via $0 \leq N \leq 1$, the magnetic susceptibility χ_{m} turns out to have the range of values $-\infty < \chi_{\mathrm{m}} \leq -1$.

Another point of view is provided by the following consideration. From (2.22) we read off that both the external magnetic field H and the stray field $H_{\mathrm{s}} = -NM$ yield an effective inner magnetic induction B_{eff}:

$$B_{\mathrm{eff}} = \mu_0 (H + H_{\mathrm{s}}) = \mu_0 (H - NM) \, . \tag{2.25}$$

Inserting therein (2.23) we obtain

$$B_{\mathrm{eff}} = \mu_0 \, \frac{1}{1-N} \, H \, . \tag{2.26}$$

In case of $N = 0$ the effective inner magnetic induction $B_{\mathrm{eff}}(H)$ coincides with the external magnetic induction $\mu_0 H$. But in case of $0 < N < 1$ the effective inner magnetic induction $B_{\mathrm{eff}}(H)$ is larger than the external magnetic induction $\mu_0 H$. For instance, for a sphere with $N = 1/3$ we obtain from (2.26)

$$B_{\mathrm{eff}}^{(\mathrm{sphere})}(H) = \mu_0 \, \frac{3}{2} \, H \, . \tag{2.27}$$

Furthermore, we observe that the effective inner magnetic induction (2.26) and the magnetization M from (2.23) are related via

$$B_{\mathrm{eff}} = -\mu_0 M \, . \tag{2.28}$$

Consequently, we conclude on formal grounds in analogy to (2.10):

$$\chi_{\mathrm{m,eff}} = \mu_0 \, \frac{\partial M}{\partial B_{\mathrm{eff}}} = -1 \, . \tag{2.29}$$

Thus, introducing the effective magnetic induction B_{eff} allows to describe also a finite probe via an effective complete diamagnetism.

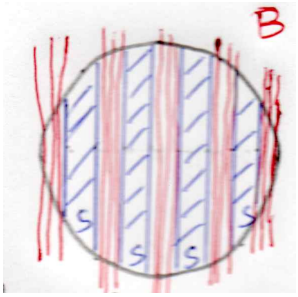

Figure 2.8: Intermediate state of type I superconductor with many flux quanta.

normal conducting region	$B_{\rm n} = \mu_0 H \geq B_{\rm c}$	$M_{\rm n} = 0$
superconducting region	$B_{\rm s} = 0$	$M_{\rm s} = -\dfrac{1}{1-N} H$

Table 2.3: Magnetic properties of normal and superconducting region for intermediate state of type I superconductor.

2.4.3 Intermediate State:

A consistency problem emerges when the effective magnetic induction $B_{\rm eff}$ in (2.26) inside the probe reaches the external critical field $B_{\rm c} = \mu_0 H_{\rm c}$:

$$\mu_0 H_{\rm c} = \mu_0 \frac{1}{1-N} H_{\rm c} \qquad \Rightarrow \qquad 1 = \frac{1}{1-N} \,. \tag{2.30}$$

Obviously (2.30) can not be fulfilled for $0 < N \leq 1$. This means that a homogeneous superconducting state is no longer possible. But on the other hand, a homogeneous normal conducting state is also not possible as this would imply $\chi_{\rm m} = M = 0$ in contradiction to (2.24). This dilemma was solved by Peirls and Landau in 1936 by concluding that neither a homogeneous superconducting nor a homogeneous normal conducting state exists at $B_{\rm eff} = B_{\rm c}$. Instead, at $B_{\rm eff} \geq B_{\rm c}$ the probe realizes an inhomogeneous intermediate state, where the probe is divided into normal and superconducting regions as follows:

1. At $B_{\rm eff} = B_{\rm c}$ the normal conducting regions occur at first at the equator and then continue from there into the inner of the probe, see Fig. 2.8. The reason for this is that the s-n border area, and thus the energy to create it, is minimal at the equator.

2. The phase boundaries between normal and superconducting regions are always parallel to the magnetic field.

3. The whole structure of the intermediate state follows from minimizing the total energy. This has two consequences:

   (a) At $B_{\rm eff} \geq B_{\rm c}$ only few s-n border areas exist, thus the coexisting normal and superconducting regions are larger. Whereas a type II superconductor has only one flux

quantum for one flux line, the normal conducting regions of the intermediate state of a type I superconductor involve hundred thousands of flux quanta.

(b) To be more precise, the intermediate state does not exactly emerge at $B_{\text{eff}} = B_{\text{c}}$ but at a slightly larger magnetic field as a certain magnetic field energy is necessary to create the s-n border areas. But in the following we neglect this additional effect for the sake of simplicity.

The normal and the superconducting region of the intermediate state are characterized by different magnetic properties as is summarized in Tab. 2.3. Thus, for an inhomogeneous intermediate state one can only talk about spatially averaged magnetic quantities. This allows us now to define an averaged magnetization for the probe response as follows. The homogeneous superconducting state is characterized due to the Meissner-Ochsenfeld effect by the magnetization (2.23) and the effective magnetic induction $B_{\text{eff}}(H)$ in (2.26). The transition point to the intermediate state is now given by that magnetic field $H_{\text{cI}} \leq H_{\text{c}}$, which fulfills

$$B_{\text{eff}}(H_{\text{cI}}) = \mu_0 H_{\text{c}} \,. \tag{2.31}$$

Thus, inserting (2.26) into (2.31) yields the initial magnetic field

$$H_{\text{cI}} = (1 - N) H_{\text{c}} \,. \tag{2.32}$$

It is, indeed, smaller than or equal to H_{c} due to the range of values of the demagnetization, i.e. $0 \leq N \leq 1$. Furthermore, the initial magnetization at the onset of the intermediate state follows from (2.23) and (2.32):

$$M_{\text{cI}} = -\frac{1}{1-N} H_{\text{cI}} = -H_{\text{c}} \,, \tag{2.33}$$

which is independent of the demagnetization N. We now describe the magnetic properties of the inhomogeneous intermediate state. As we have there both normal and superconducting regions, the effective magnetic induction (2.25) has to be generalized to

$$\tilde{B}_{\text{eff}}(H) = \mu_0 \left(H - N \tilde{M} \right) \,. \tag{2.34}$$

Here the tilde denotes explicitly the spatial averaging procedure. And the intermediate state is now characterized by the condition that this spatially averaged magnetic induction (2.34) is determined by the initial magnetic field:

$$\tilde{B}_{\text{eff}}(H) = \mu_0 H_{\text{c}} \,. \tag{2.35}$$

Thus, combining (2.34) and (2.35) yields for the averaged magnetization

$$\tilde{M}(H) = \frac{H - H_{\text{c}}}{N} \,. \tag{2.36}$$

On the one hand, we recognize that (2.36) reproduces with (2.32) the magnetization (2.33) at the onset of the intermediate state:

$$\tilde{M}(H_{\text{cI}}) = -H_{\text{c}} \,. \tag{2.37}$$

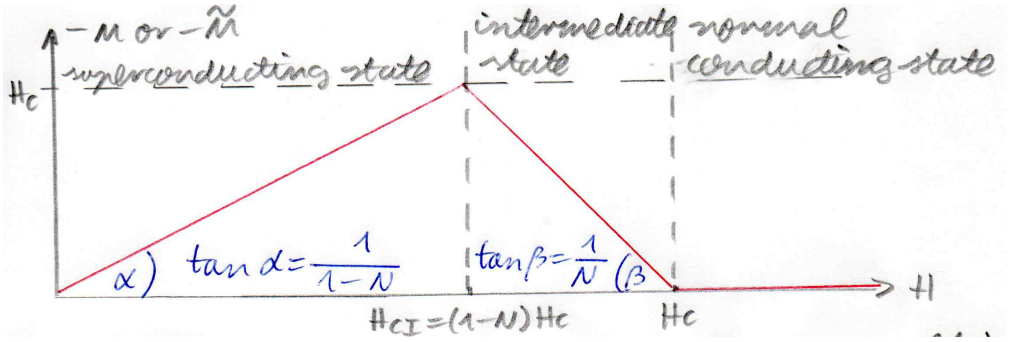

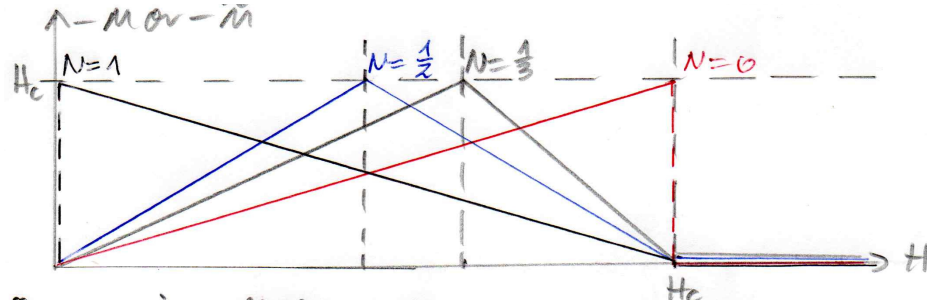

Figure 2.9: Negative Magnetization as function of magnetic field for intermediate state of type I superconductor: a) Generic case, b) Special cases for different values of the demagnetization factor N.

On the other hand, we read off from (2.36) that the averaged magnetization $\tilde{M}(H)$ vanishes at $H = H_\mathrm{c}$:

$$\tilde{M}(H_\mathrm{c}) = 0\,, \tag{2.38}$$

which describes the transition of the intermediate state to the normal conducting state. The resulting generic magnetization curve is depicted in Fig. 2.9a). For different demagnetization factors N one obtains different magnetization curves as is illustrated in Fig. 2.9b). The shown cases correspond to the infinitely thin layer ($N = 1$), the infinitely long cylinder ($N = 1/2$), the sphere ($N = 1/3$), and an infinitely large probe ($N = 0$), where no surface effects occur. Comparing all those demagnetization curves in Fig. 2.9b), we recognize that the areas below the triangles are equal. As all triangles have the same base line H_c and the same height H_c their resulting area amounts to $H_c^2/2$. This area corresponds to the energy difference between the superconducting and the normal conducting phase. It turns out to be independent of the demagnetization factor N and, thus, independent of the probe shape:

$$E_\mathrm{n} - E_\mathrm{s} = -\mu_0 V \int_0^{H_\mathrm{c}} M(H) dH = \frac{\mu_0}{2} V H_\mathrm{c}^2 = \frac{B_\mathrm{c}^2}{2\mu_0} V\,. \tag{2.39}$$

Thus, the superconducting state has a lower magnetic energy, which is called condensation energy. In the microscopic picture of the BCS theory, this energy gain results from the condensation of single electrons at the surface of the Fermi sphere to Cooper pairs.

Now we determine the corresponding magnetic induction B. Due to the Meissner-Ochsenfeld effect (2.6) it vanishes in the superconducting state. In the inhomogeneous intermediate state the spatially averaged magnetic induction reads in analogy to (2.22):

$$\tilde{B} = \mu_0 \left[H + (1 - N)\tilde{M} \right] . \tag{2.40}$$

Inserting (2.36) into (2.40) then yields

$$\tilde{B} = \mu_0 \left[\frac{1}{N} H + \left(1 - \frac{1}{N} \right) H_\mathrm{c} \right] . \tag{2.41}$$

Thus, at the onset of the intermediate state we obtain with (2.32) and (2.41) an agreement with the Meissner-Ochsenfeld effect:

$$\tilde{B}(H_\mathrm{cI}) = 0 . \tag{2.42}$$

Furthermore, we find at H_c due to (2.41)

$$\tilde{B}(H_\mathrm{c}) = \mu_0 H_\mathrm{c} , \tag{2.43}$$

so that the magnetic induction goes over continuously into the one of the normal conducting state

$$B(H) = \mu_0 H . \tag{2.44}$$

Thus, we can summarize these findings in the generic demagnetization curve shown in Fig. 2.10a). For different demagnetization factors N these magnetization curves have the form depicted in Fig. 2.10b).

2.5 Experiments

Here we briefly review three breakthrough experiments, which allowed to investigate the peculiar magnetic properties of superconductors.

2.5.1 Iron Colloids

According to the experimental set-up sketched in Fig. 2.11, above a superconducting probe iron is vaporized from a hot wire. The iron atoms diffuse through the helium gas of the cryostate, which stabilizes the temperature in the Kelvin regime and build iron colloids. Those colloids have a diameter of smaller than 50 nm and sediment in helium slowly at the surface of the superconductor. The ferromagnetic iron colloids accumulate at the normal conducting regions as there the magnetic field is largest. And, finally, the iron colloids are visualized with an electron microscope.

With this experimental procedure Eßmann and Träuble could detect at the Max-Planck Institute of Solid-State Physics in Stuttgart in 1966 the intermediate state in superconductors of type I and in 1968 the flux lattice of the mixed state in superconductors of type II.

a)

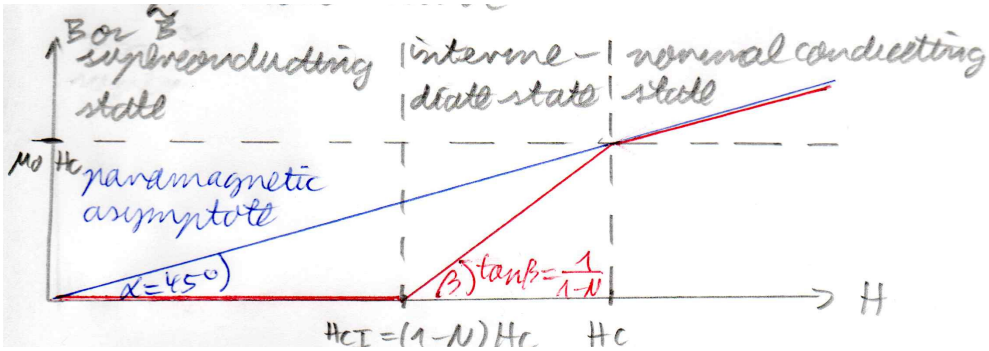

b)

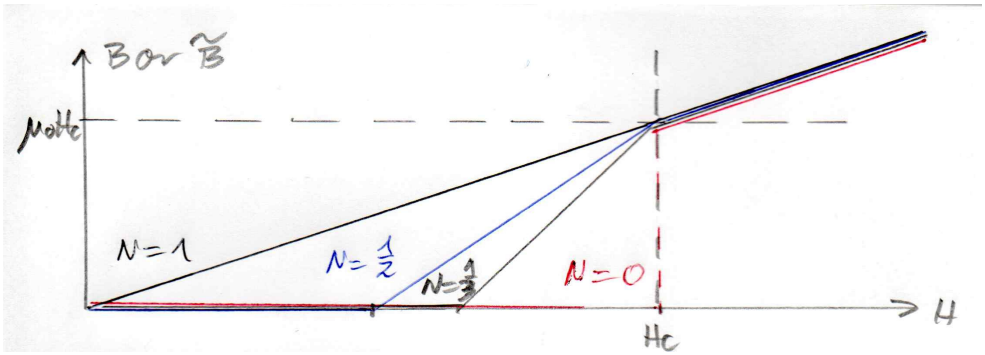

Figure 2.10: Demagnetization curves of type I superconductor including the intermediate state: a) Generic case and b) for different demagnetization factors N.

2.5.2 Niobium Powder

Another method is based on investigating a superconducting probe in the intermediate state with a fine powder of a superconducting material. Which requirements follow for both the probe and the powder? Most importantly, the powder must be superconducting when the type I superconductor is in the intermediate state. This requires the magnetic field of the powder to be larger than the critical magnetic field of the probe:

$$B_{\mathrm{c}}(\text{probe}) < B_{\mathrm{c}}(\text{powder})\,. \tag{2.45}$$

Due to the Kok approximation of the transition line (1.3) in the B-T phase diagram this implies that the critical temperature of the powder must be larger than the critical temperature of the probe:

$$T_{\mathrm{c}}(\text{probe}) < T_{\mathrm{c}}(\text{powder})\,. \tag{2.46}$$

As the critical temperature of niobium with $T_{\mathrm{c}} = 9.2\,\mathrm{K}$ is larger than the critical temperature of many other superconductors, one uses quite often niobium powder.

The small grains of the niobium powder represent ideal diamagnets in the superconducting state. Therefore, they are expelled from the regions of larger magnetic fields, i.e. the normal conducting regions. Thus, they gather preferably at the surface of superconducting regions.

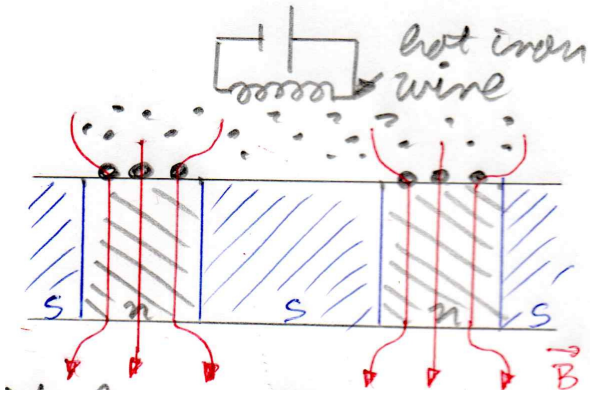

Figure 2.11: Experimental set up to detect normal conducting regions of a type I superconductor with iron colloids.

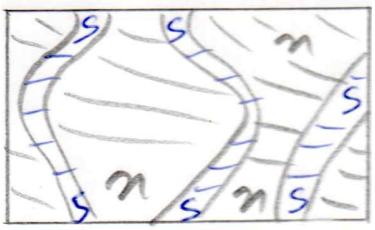

Figure 2.12: Experimental set up to detect superconducting regions of a type I superconductor with niobium powder.

A view from the top on a planar prom then reveals meandering superconducting regions as is shown in Fig. 2.12.

2.5.3 Faraday Effect

The Faraday effect is a magneto-optical phenomenon, i.e. it originates from an interaction between light and magnetic field in a medium. More precisely, the Faraday effect causes a rotation of the plane of the polarization, which is linearly proportional to the component of the magnetic field in the direction of the propagation.

In order to observe the Faraday effect experimentally, one uses crossed polarizers. Without a magnetic field, the observed light intensity behind the crossed polarizers vanishes. But with a magnetic field in the propagation direction of light, the observed light intensity no longer vanishes. But one can rotate one polarizer with a certain angle α, so that the light vanishes again. And this angle α turns out to be not only proportional to the magnetic induction B in propagation direction but also to the material width d:

$$\alpha = V\, dB\,. \tag{2.47}$$

Here V denotes the Verdet constant, which is determined by the dispersion $dn/d\lambda$ of the

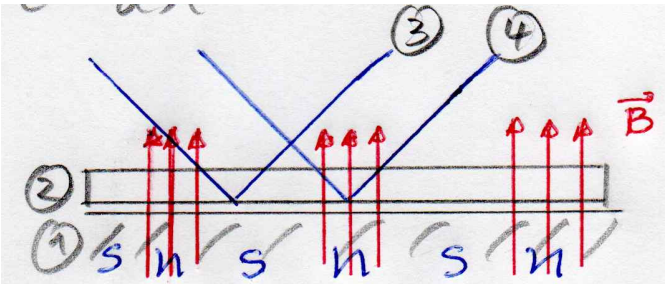

Figure 2.13: Experimental set up to detect normal conducting regions of a type I superconductor with the Faraday effect.

underlying material:

$$V = -\frac{e\lambda}{2mc}\frac{dn}{d\lambda}\,. \tag{2.48}$$

Here n denotes the refractive index and λ the wave length of light. Thus, we conclude that the Faraday effect is largest in the vicinity of an absorption line, as then the dispersion $dn/d\lambda$ is largest. This absorption allows an atomistic interpretation of the Faraday effect. In the vicinity of an absorption line the electrons oscillate resonantly with the light frequency in the polarization direction. Thus, in presence of an additional magnetic field in propagation direction, a Lorentz force acts on the electrons, which causes them to precess with the Larmor frequency

$$\omega_{\mathrm{L}} = \frac{eB}{2m}\,. \tag{2.49}$$

And this precession causes the polarization plane to rotate with an angle α, which can also be rewritten according to (2.47)–(2.49) via

$$\alpha = -\omega_{\mathrm{L}}\, d\, \frac{\lambda}{c}\frac{dn}{d\lambda}\,. \tag{2.50}$$

The experimental set up looks now as visualized in Fig. 2.13. Here ① represents a superconductor, whose surface is formed to be a mirror. On top of ① we have a magneto-optical active material ②. Is the light beam reflected at a superconducting mirror region ③, there is no magnetic induction due to the Meissner-Ochsenfeld effect and the polarization plane is not changed. But if the light beam is reflected at a normal conducting region of the mirror ④, the magnetic induction there yields a rotation of the polarization direction. In conclusion, the Faraday effect allows to distinguish between superconducting and normal conducting regions at the surface of the superconductor. One advantage of the Faraday effect in comparison with the powder method is that it also allows to detect, in principle, temporal changes of the intermediate state of type I superconductors.